厚生労働省科学研究委託費（革新的がん医療実用化研究事業）
委託業務成果報告（業務項目：付随研究）

臨床試験、発症ハイリスクコホート、ゲノム解析を統合したアプローチによるATL標準治療法の開発に関する研究

担当責任者 森下　和広　宮崎大学医学部　教授

研究要旨：成人T細胞白血病(ATL)40−50%に皮膚症状が伴い、それは各種特異疹として、その多くはATL細胞の浸潤とされている。この皮膚症状はindlentタイプのATLに伴って発見されているがそれが臨床的に特別な病型であるのか、明らかにされていない。そこで皮膚症状を伴うATLのゲノム解析を行い、その臨床病型としての意味付けを検討する。本年度は皮膚症状を伴うくすぶり型ATL７症例についてエクソームシークエントとSNPアレイゲノムコピー数解析を行い、皮膚浸潤に特異的なゲノム増幅、欠失領域を同定した。さらなる解析により、遺伝子異常の同定、機能解析につなげる予定である。

A. 研究目的

成人T細胞白血病(ATL)40−50%に皮膚症状があり、各種特異疹として、その多くはATL細胞の浸潤とされている。Indolentタイプの ATLに皮膚浸潤があった場合の臨床的に特別な病型として成り立つのか否かの判断がついておらず、またその関連因子もわかっていない。そこで皮膚浸潤をきたすATLのゲノム解析を行うことで、皮膚浸潤と遺伝子異常の関係を検討し、その機能解析からその予後予測や臨床病型としての意味付けを検討する。

B. 研究方法

宮崎大学医学部附属病院皮膚科受信患者の中で皮膚浸潤を伴うATL患者において、末梢血中HTLV-1感染細胞としてTSLC1+CD4+リンパ球を分離し、ゲノムDNA、RNAを採取、高密度SNPアレイ解析、exome sequence、発現アレイ解析を行う。これらの結果を統合し、皮膚浸潤に特異的なゲノム異常、遺伝子発現以上を同定し、その機能解析を通じて、診断法の確立、予後との関連性、治療法の開発につなげる。

（倫理面への配慮）

ATL患者検体について、宮崎大学医学部A(ATL)に特異的な細胞因子と腫瘍化の検討について、2014-067 承認番号 972 号)のもと、患者情報の保護並びにヘルシンキ条約に基づき適正に処理されている。

C. 研究結果

皮膚症状を伴うATLのゲノム異常を明らかにするために、宮崎大学付属病院皮膚科において皮膚型と診断されたATL（下山分類ではくすぶり型）を対象に、エクソームシーケンシングおよびSNPアレイCGH解析を行った。皮膚型は皮膚症状により、丘疹・紅斑型と小結節・腫瘤型に分類され、解析に用いた７検体のうち、丘疹・紅斑型が４例、小結節型が２例、１名不明となっている。また、末梢血におけるTSLC1+CD4+細胞の割合は20-40%、プロウイルス量、白血球数やLDHなどの予後因子は典型的なくすぶり型を呈している。

検体として、患者から採取した血液を比重遠心分離に供し、末梢血単核球を分離、TSLC1磁気ビーズによりTSLC1陽性ATL細胞を単離し、ゲノムDNAを抽出、解析に用いた。SNPアレイ解析は、６例（丘疹・紅斑型、４例、小結節型２例）に対して行った。その結果、全６例のうち２例以上（約３割以上）に共通して見られる染色体異常を10領域同定し、増幅として、

7q32.3, 7q36.1-3, 10p11.21-22, 13q21.31, 22q11.22-q11.23、欠失に、1q31.3, 7p14.1, 7q34, 9p23, 14q11.2 を見出した。丘疹・紅斑型では、7q36.1-2, 14q32.33, 22q11.22-q11.23 の増幅、および 7p14.1, 7q34, 9p23, 14q11.2 の欠失が半数以上の症例において見られた。一方、小結節型では、22q11.22-q11.23 の増幅が共通に見られた。ホモ欠失としては、7p14.1（２例），14q11.2（３例）を同定した。7p14.1, 7q34, 14q11.2 の領域は、急性型 ATL においても共通欠失領域として同定している一方で、22q11.22-q11.23 の増幅は、皮膚型に特異的かつ全症例に見られることから、皮膚症状の病態との関連性が示唆される。今回同定した領域に存在する遺伝子の発現解析については、今後の課題である。

エクソームシーケンシングの解析は、上述の７例を用いて行い、その結果、TSLC1 陽性 ATL 細胞において、３例以上に共通して見られる１塩基置換として１１４種を同定し、７例共通では１４種の１塩基置換を同定した。これらのうち、丘疹・紅斑型特異的な塩基置換としては１３種あり、小結節型に特異的なものでは、１６種存在した。現在、コントロールとして解析した TSLC1 陰性分画のデータを用いて、ATL 細胞特異的な１塩基置換の抽出、整理を行っている。

D. E.　考察と結論

SNP アレイ解析により、皮膚症状を伴う ATL に特異的なゲノム増幅領域を同定した。さらに、遺伝子発現解析、並びにエクソームシーケンシング解析および SNP アレイ解析とも、今後検体数を増やして行くことで、丘疹・紅斑型と小結節・腫瘤型の異なる症状を示す皮膚症状を伴う ATL を特徴づけるゲノム異常を解き明かして行きたいと考えている。

F. 健康危険情報

特になし

G. 研究発表

1.　論文発表

英文雑誌

1. Nakahata S, Morishita K. PP2A inactivation by ROS accumulation. Blood, 124:2163-5, 2014.
2. Yamasaki M, Harada E, Tamura Y, Lim SY, Ohsuga T, Yokoyama N, Morishita K, Nakamura K, Ohta H, Takiguchi M. In vitro and in vivo safety and efficacy studies of amphotericin B on Babesia gibsoni. Vet Parasitol, 205:424-33, 2014.
3. Yamasaki M, Nishimura M, Sakakibara Y, Suiko M, Morishita K, Nishiyama K. Delta-tocotrienol induces apoptotic cell death via depletion of intracellular squalene in ED40515 cells. Food Funct, 5:2842-9, 2014.
4. Miyauchi S, Umekita K, Hidaka T, Umeki K, Aratake Y, Takahashi N, Sawaguchi A, Nakatake A, Morinaga I, Morishita K, Okayama A. Increased plasma lactoferrin levels in leucocytapheresis therapy in patients with rheumatoid arthritis. Rheumatology (Oxford), 53:1966-72, 2014.
5. Nagai K, Nakahata S, Shimosaki S, Tamura T, Kondo Y, Baba T, Taki T, Taniwaki M, Kurosawa G, Sudo Y, Okada S, Sakoda S, Morishita K. Development of a complete human anti-human transferrin receptor C antibody as a novel marker of oral dysplasia and oral cancer. Cancer Med, 3:1085-99, 2014.

6. Kai H, Akamatsu E, Torii E, Kodama H, Yukizaki C, Akagi I, Ino H, Sakakibara Y, Suiko M, Yamamoto I, Okayama A, Morishita K, Kataoka H, Matsuno K. Identification of a bioactive compound against adult T-cell leukemia from bitter gourd seeds. Plants, 3:18-26, 2014.
7. Nakahata S, Ichikawa T, Maneesaay P, Saito Y, Nagai K, Tamura T, Manachai N, Yamakawa N, Hamasaki M, Kitabayashi I, Arai Y, Kanai Y, Taki T, Abe T, Kiyonari H, Shimoda K, Ohshima K, Horii A, Shima H, Taniwaki M, Yamaguchi R, Morishita K. Loss of NDRG2 expression activates PI3K-AKT signalling via PTEN phosphorylation in ATLL and other cancers. Nature Comm, 5: 3393, 2014.
8. Nagahama K, Eto N, Sakakibara Y, Matsusita Y, Sugamoto K, Morishita K, Suiko M. Oligomeric proanthocyanidins from rabbiteye blueberry leaves inhibits the proliferation of human T-cell lymphotropic virus type 1-associated cell lines via apoptosis and cell cycle arrest_Journal of Functional Foods, 6:356–366, 2014.

2. 学会発表

1. New therapeutic approach using anti-human ITGA6/B4 neutralizing antibody for EVI1 high AML Kaneda K, Suekane A, Kurosawa G, Sudo Y, Furuya A, Morishita K. (TENTH INTERNATIONAL WORKSHOP Cincinnati Children's Hospital Medical Center, May.4-7,2014. (ポスター)
2. 中武彩子、小林行治、中畑新吾、西片一朗、岩永正子、相良康子、北中明、天野正宏、前田宏一、末岡栄三朗、瀬戸山充、岡山昭彦、宇都宮與、下田和哉、渡邊俊樹、森下和広:血中可溶性CADM1/TSLC1 測定による ATL 診断法の開発,第 1 回日本 HTLV-1 学会学術集会,港区,2014 年 8 月 24 日.(口演)
3. 西片一朗、市川朝永、中畑新吾、藤井雅寛、伊波英克、白神俊幸、田中勇悦、井上純一郎,森下和広:ATL 細胞における CADM1 高発現に必須な NF-ｋB 活性化には新規制御因子ｐ47 の発現低下が関係する,第 1 回日本 HTLV-1 学会学術集会,港区,2014 年 8 月 24 日.(口演)
4. 市川朝永、中畑新吾、森下和広:ATL における新規 PTEN キナーゼの同定と機能解析,第 1 回日本 HTLV-1 学会学術集会,港区,2014 年 8 月 23 日～25 日.(ポスター)
5. 市川朝永、中畑新吾、藤井雅寛、伊波英克、森下和広:NDRG2 は PPA2 を介して NIK 活性を制御し、恒常的 NF-ｋB 活性を抑制する,第 73 回日本癌学会学術総会,横浜,2014 年 9 月 25 日.(口演)
6. 森下和広、中畑新吾、市川朝永:NDRG2 は PPA2 と共に HTLV-1 感染による活性化 PI3K/AKT と NF-ｋB 情報伝達を阻害する,第 73 回日本癌学会学術総会,横浜,2014 年 9 月 25 日.(口演)
7. 末金彰、兼田加珠子、ManachaiNawin、森下和広:EVI1 高発現急性骨髄性白血病における monosomy7 ゲノム異常の解析,第 73 回日本癌学会学術総会,横浜, 2014

年9月25日.（ポスター）

8. Nakahata S, Ichikawa T, Arai Y, Taki T, Taniwaki M, Morishita K:NDRG2 S332 phosphorylation is necessary to recruit PP2A to dephosphorylate PTEN in a feedback loop in the PI3K pathway (118) PI3K系のフィードバックループにおけるNDRG2 S332のリン酸化は、PTEN脱リン酸化を誘導するPP2Aリクルートメントに必須である,第73回日本癌学会学術総会,横浜,2014年9月27日.（ポスター）
9. 田村知丈、市川朝永、中畑新吾、近藤雄大、馬場貴、長井健太郎、山下善弘、森下和広:がん抑制遺伝子NDRG2欠損マウスによる4-NQO誘導性口腔がん発症機構の解析,第73回日本癌学会学術総会,横浜,2014年9月27日.（ポスター）
10. 森下和広、中畑新吾、市川朝永:PTENリン酸化異常に伴う白血病、癌発症機構 ,第87回日本生化学会大会,京都,2014年10月18日.（口演）
11. 市川朝永、中畑新吾、森下和広:新規がん抑制遺伝子Ndrg2欠損マウスはAKT活性の亢進を介して抗うつ状態を改善する,第87回日本生化学会大会,京都,2014年10月16日.（ポスター）
12. 兼田加珠子、井川加織、太田智美、関本朝久、帖佐悦男、迫田隅男、今泉和則、ﾏﾆｻｲ･ﾌﾟﾃﾞｨ、山口良二、森下和広:骨軟骨分化におけるMEL1/PRDM16の機能解析,第87回日本生化学会大会,京都,2014年10月18日.（ポスター）
13. 中畑新吾、市川朝永、齋藤祐介、滝智彦、谷脇雅史、森下和広:ATLやその他のがんにおけるNDRG2発現低下はPTENリン酸化異常をきたし、PI3K/AKT経路を活性化させる,第76回日本血液学会学術集会,大阪,2014年11月1日.（口演）
14. Kazuko K, Suekane A, Kurosawa J, Sudo Y, Furuya A, Morishita K: Improvement therapeutic efficacy by neutralizing antibody of integrinA6/B4 for EVI1 high AML,第76回日本血液学会学術集会,大阪,2014年10月31日.（ポスター）
15. 伊波英克、池辺詠美、越海ニコール、緒方正男、手塚健太、松本昴、末岡栄三郎、堀光雄、長谷川寛雄、森下和広、田中勇悦、藤沢順一、紙健次郎:細胞外排出低分子量メタボライトの定量によるATL細胞のプロファイリング,第37回日本分子生物学会年会,神奈川,2014年11月25日.（ポスター）
16. 中畑新吾、市川朝永、新井康仁、滝智彦、谷脇雅史、森下和広:PI3Kシグナルによるエンドサイトーシス制御に関与する分子の探索,第37回日本分子生物学会年会,神奈川,2014年11月27日.（ポスター）
17. 市川朝永、中畑新吾、森下和広:PTENリン酸化異常におけるATLがん発症機構（第19回造血器腫瘍研究会ﾌﾟﾛｸﾞﾗﾑ,佐賀県,2015年1月23日.（口演）

H. 知的財産権の出願・登録状況

特になし

厚生労働省科学研究委託費（革新的がん医療実用化研究事業）
委託業務成果報告（業務項目：付随研究）

臨床試験、発症ハイリスクコホート、ゲノム解析を統合したアプローチによるATL標準治療法の開発に関する研究

担当責任者　天野　正宏　宮崎大学医学部　准教授

研究要旨：くすぶり型、慢性型 ATLL の急性転化前後の皮膚浸潤病変からゲノム解析をおこない、悪化進行に関連する因子の解明をおこなう。

A. 研究目的

宮崎大皮膚科では皮膚浸潤を有するATLL を診療している。日常臨床では、紅斑、丘疹を伴うくすぶり型 ATLL は、進行とともに結節、腫瘤へ皮膚浸潤が悪化し、また局所に限局していた結節、腫瘤も進行とともに多発してくることをよく経験する。この時期には末梢血やLDH 値で大きな変化もないため、皮膚症状は採血データで現れないATLL の進行を早めに把握できると考えられる。またくすぶり型 ATLL では、皮膚に生じた腫瘤は放射線治療をおこない治療することが多い。時に放射線治療後、一時的ではあるが照射範囲以外の紅斑、丘疹、結節も同時に縮小する現象、いわゆるアブスコパル効果をみることがある。この時期には末梢血中に腫瘍抑制物質が発現していることが予想され、この物質を特定することは、今後の ATLL 治療の開発に寄与するものと思われる。

B. 研究方法

皮膚浸潤を伴うくすぶり型ATLL 患者の皮膚生検をおこない、病理学的に皮膚浸潤を確認するとともに一部を凍結保存する。皮膚病変が結節、腫瘤へ皮膚浸潤が変化した場合に、再度、皮膚生検をおこない病理の確認とともに病変を凍結保存する。凍結保存した皮膚浸潤のゲノム解析をおこない進行前後での相違を比較検討する。放射線治療前後の病変の消退に関しても同様である。

（倫理面への配慮）

ヘルシンキ宣言に従って研究を実施し、患者を匿名としてプライバシー保護に配慮した。

C. 研究結果

ATLL の皮膚浸潤病変の採取について、後方視的に過去のホルマリン固定標本からレーザーマイクロダイセクションをおこない、病変部の DNA を抽出する方法が提案したが、班会議では RNA の抽出など可能な限り生標本が良いとされ、皮膚性検時に凍結保存する事となった。

D. 考察

アブスコパル効果では放射線治療により死滅した腫瘍細胞を認識した樹状細胞などが CD4+T リンパ球や CD8+T リンパ球に抗原提示をおこない、これらが腫瘍細胞を攻撃するとされている。阿久津らは放射線による heat shock protein gp96 の発現増強がアブスコパル効果に関与していることを示唆している。皮膚病変消退前後に採血を行い、heat shock protein の測定も必要である。

E. 結論

皮膚病変を有するくすぶり型ATLL の患者さんにおいて、臨床像が変化した場合に皮膚生検をおこない、半割組織を凍結保存する。また同時に採血もおこない各種臨床検査やPVL の測定、凍結保存をおこなっている。

F. 健康危険情報

G. 研究発表

1. 論文発表

英文雑誌

1. Tsukasaki K, Imaizumi Y, Tokura Y,

Ohshima K, Kawai K, Utsunomiya A, Amano M, Watanabe T, Nakamura S, Iwatsuki K, Kamihira S, Yamaguchi K, Shimoyama M. Meeting report on the possible proposal of an extranodal primary cutaneous variant in the lymphoma type of adult T-cell leukemia-lymphoma. J Dermatol, 41: 26-8, 2014.

2. Sugaya M, Tokura Y, Hamada T, Tsuboi R, Moroi Y, Nakahara T, Amano M, Ishida S, Watanabe D, Tani M, Ihn H, Aoi J, Iwatsuki K.Phase II study of i.v. interferon-gamma in Japanese patients with mycosis fungoides. J Dermatol, 41: 50-6, 2014.

和文雑誌

1. 天野正宏、前久保理恵、濱田利久、岩月啓氏:Cutaneous Lymphoma in Japan: Adult T-cell Leukemia/Lymphoma (ATLL) and Human T-lymphotropic Virus Type 1 (HTLV-1) Related Diseases. 日皮会誌 124:2561-2563, 2014.
2. 成田幸代、室井栄治、持田耕介、加嶋亜紀、天野正宏、瀬戸山充:肺癌および胃原発成人 T 細胞白血病/リンパ腫を合併した皮膚筋炎の 1 例. 西日皮膚 76:550-554,2014.

2. 学会発表

1. Amano M, Inoue T, Horikawa N , Setoyama M . CONCURRENT LENTIGO MALIGNA MELANOMA AND CUTANEOUS T-CELL LYMPHOMA IN A 62 YEAR-OLD MAN. 3rd Eastern Asia Dermatology Congress, 韓国済州島,2014 年 9 月 24 日～26 日. (ポスター)
2. 天野正宏、前久保理恵、濱田利久、岩月啓氏:Cutaneous Lymphoma in Japan: Adult T-cell Leukemia/Lymphoma (ATLL) and Human T-lymphotropic Virus Type 1 (HTLV-1) Related Diseases, 第 113 回日本皮膚科学会総会教育講演 10 「アジアのリンパ腫」,京都 ,2014 年 5 月 30 日. (口演)
3. 天野正宏、飯川まどか、成田幸代、堀川永子、瀬戸山充:消化管浸潤をともなった Adult T-cell leukemia/lymphoma(ATLL)の 3 例,日本皮膚科学会第 368 回福岡地方会 中山樹一郎皮膚科主任教授退任記念,福岡, 2014 年 3 月 15 日. (口演)

H. 知的財産権の出願・登録状況
(予定を含む)

1. 特許取得

特になし。

2. 実用新案登録

特になし。

3. その他

特になし。

厚生労働省科学研究委託費（革新的がん医療実用化研究事業）
委託業務成果報告（業務項目：付随研究）

臨床試験、発症ハイリスクコホート、ゲノム解析を統合したアプローチによるATL標準治療法の開発に関する研究

担当責任者　戸倉　新樹　浜松医科大学皮膚科学講座　教授

研究要旨：病変皮膚を用いたATL腫瘍細胞のバイオマーカーの検討

A. 研究目的

成人T細胞性白血病・リンパ腫（ATL）患者の約50%は皮膚病変を伴う。皮膚病変が生じやすい機構は，病理学的に表皮向性（epidermotropism）と呼ばれる腫瘍細胞の皮膚とくに表皮に向かって浸潤する性質による。その皮膚病変は臨床的に、斑型（patch type），局面型（plaque type），結節・腫瘤型（nodulotumoral type），紅皮症型（erythrodermic type），多発丘疹型（multipapular type），紫斑型（purpuric type）の6型に分けることができる（Sawada Y et al. Blood 2011）。

皮膚の effector/memory T cells は cutaneous lymphocyte anigen (CLA)を発現し、このCLA発現皮膚ホーミングT細胞が真皮後毛細血管内に発現するE-selectinと相互作用する。こうしたCLA陽性細胞は同時に特異的にTh2 chemokine receptorであるCC-chemokine receptor 4 (CCR4)を共発現し、そのリガンドであるCC-chmeokine ligand 17 (CCL17, TARC)とCCL22 (MDC)に結合する。これら接着因子、ケモカイン／ケモカインレセプターとの相互作用がeffector/memory T cellsの真皮、表皮へのホーミングに必要不可欠とされる。

一方ATLに関しても同様の知見が得られている。ATL細胞のほとんどが、CCR4を発現していることが明らかとなっている。さらに、ATL細胞で皮膚に浸潤している細胞の多くが、$CCR4^{+}CXCR3^{-}CLA^{+}CD4^{+}$であり、かつ$CCR4^{+}$ acute ATLの方が、$CCR4^{-}$ acute ATLより予後が悪いと報告した。我々も、CD4/8 double negativeなATLでもCCR4を表面抗原に持つ症例を経験している。また、末梢血および皮膚に浸潤するATL細胞はCCR4を発現し、皮膚に腫瘤を形成する症例でそのligandsであるTARC, MDCをATL自らが産生することを証明した（Shimauchi T et al: Clin Cancer Res 2005）。以上から、Th2 chemokine receptorであり、かつ皮膚ホーミングレセプターであるCCR4の発現は皮膚に出現するリンパ腫において重要なレセプターであるといえる。

以上のようにATLの皮膚浸潤及びその細胞生物学的態度はケモカイン／ケモカイン受容体に影響を受ける。その他に、PD-1/PD-L1、Notch signaling、TSLC1/CADM1、Caveolin-1、HBZ (HTLV-1 bZIP factor)など、皮膚浸潤ATL細胞の動態を反映するバイオマーカーの候補がある。ここでは、そうした分子発現について検討した。

B. 研究方法

用いる皮膚検体は、1) 単離した細胞、2) 皮膚生（なま）検体、3) パラフィン切片とした。

単離した細胞は、フローサイトメトリーによる細胞表面形質、培養上清中物質，RT-PCR，microRNAに供した。皮膚生検体は、免疫染色，RT-PCR，microRNAの解析に用いた。パラフィン切片は、免疫染色やゲノム解析に用いた。

PD-1/PD-L1、Notch signaling、TSLC1/CADM1について中心的に研究を行うこととした。

C. 研究結果

PD-1/PD-L1について、我々はすでに、皮膚や末梢血から得られたATL細胞がPD-1のみならずPD-L1を発現することを報告している（Shimauchi T et al. Int J Cancer

2007)。PD-L1 の発現が特に重要であることを確認した。ATL 細胞に発現した PD-L1 は、bystander な CD4 あるいは CD8 陽性正常 T 細胞に働きかけ、それら細胞の機能低下をもたらし、免疫不全状態を誘導すると考えられた。

Notch signaling については現在パラフィン切片を染色することにより、その発現を皮疹型の違いによって解析している。

TSLC1/CADM1 発現は、菌状息肉症や Sézary 症候群と比較検討した。こうした皮膚 T 細胞リンパ腫においても CADM1 を発現することが明らかになり、ATL との発現パターンについて検討を継続している。

D. 考察

皮膚浸潤 ATL 細胞は、CCR4 発現、PD-L1 発現などにおいて末梢血 ATL 細胞より顕著な特徴を持つ可能性が示された。今後 Notch signaling や CADM1 発現についてさらなる検討を行いたい。

E. 結論

ATL の皮膚浸潤腫瘍細胞は、より性格付けが顕著な分子発現を行っており、活性化した状態を保持していると考えられる。

F. 健康危険情報

なし

G. 研究発表

1. 論文発表

英文雑誌

1. Tokura Y, Sawada Y, Shimauchi T. Skin manifestations of adult T-cell leukemia/lymphoma: Clinical, cytological, and immunological features. J Dermatol, 41: 19-25, 2014.
2. Sugaya M, Tokura Y, Hamada T, Tsuboi R, Moroi Y, Nakahara T, Amano M, Ishida S, Watanabe D, Tani M, Ihn H, Aoi J, Iwatsuki K. Phase II study of intravenous interferon-γ in Japanese patients with mycosis fungoides. J Dermatol, 41: 50-56, 2014.
3. Hoshino T, Tatsuno K, Shimauchi T, Okada S, Ito T, Ono T, Ohshima K, Tokura Y. Epstein-Barr virus-associated T-cell lymphoproliferative disorder affecting skin and lung in an elderly patient. J Dermatol, 41: 837-840, 2014.
4. Kasuya A, Yagyu T, Tokura Y. Recurrent herpes zoster on a fixed thigh site: Its possible association with lymphoma cell invasion to femoral nerve. J Dermatol, 41: 854-855, 2014.

2. 学会発表

1. Tokura Y. Adult T-cell leukemia/lymphoma (ATLL): Immunosuppresive chracteristics of tumor cells. Dermatology Seminar. Cardiff, UnitedKingdom, May.23, 2014. (口演)
2. Shimauchi T, Blanchet F, Ladell K, Price D, Bangham C, Tokura Y, Piguet V: Dendritic cells-T cells virological syanapse formation contributes to the Human T-cell Leukemia Virus type 1 infection as well as functional suppression on dendritic cells. 44th Annual Meeting of the European Society for Dermatological Research, Copenhagen, Denmark.Nov.11-13, 2014. (口演)

H. 知的財産権の出願・登録状況

(予定を含む)

1. 特許取得

なし

2. 実用新案登録

なし

3. その他

なし

学 会 等 発 表 実 績

委託業務題目　「 臨床試験、発症ハイリスクコホート、ゲノム解析を統合したアプローチによるATL標準治療法の開発に関する研究」

機関名　国立がん研究センター東病院

1．学会等における口頭・ポスター発表

発表した成果（発表題目、口頭・ポスター発表の別）	発表者氏名	発表した場所（学会等名）	発表した時期	国内・外の別
本邦における慢性・くすぶり型ATLの後方視的解析.（口演）	勝屋弘雄、石塚賢治、天野正宏、河井一浩、日野亮介、宇都宮與、花田修一、山中竹春、鈴宮淳司、田村和夫	福岡（第12回日本臨床腫瘍学会学術集会）	2014年7月17日～19日	国内
Adult T-cell leukemia/lymphoma (ATLL): Immunosuppresive chracteristics of tumor cells.（口演）	Tokura Y	Dermatology Seminar	2014年5月23日	国外
A nationwide survey of patients with adult T cell leukemia/lymphoma (ATL) in Japan: 2010-2011.（口演）	野坂生郷、岩永正子、石澤賢一、石田陽治、内丸薫、石塚賢治、天野正宏、石田高司、今泉芳孝、鵜池直邦、宇都宮與、大島孝一、河井一浩、田中淳司、戸倉新樹、飛内賢正、渡邉俊樹、塚崎邦弘	大阪（第76回日本血液学会）	2014年10月31日～11月2日	国内
血中可溶性CADM1/TSLC1測定によるATL診断法の開発.（口演）	中武彩子、小林行治、中畑新吾、西片一朗、岩永正子、相良康子、北中明、天野正宏、前田宏一、末岡栄三朗、瀬戸山充、岡山昭彦、宇都宮與、下田和哉、渡邊俊樹、森下和広	東京（第1回日本HTLV-1学会学術集会）	2014年8月24日	国内
Is watch and wait still standard for indolent ATL?（口演）	Ishitsuka K	San Francisco（7Th annual T-cell lymphoma forum）	2015年1月29日～31	国外

Hierarchical clustering analysis of surface antigens on ATL cells and search for AT- initiating cell marker.（ポスター）	Ishigaki T, Kobayashi S, Nakano N,Utsunomiya A, Uchimaru K , Tojo A	横浜（第73回日本癌学会学術総会）	2014年9月25日～27日	国内
Comprehensive Analysis of Surface Antigens on Adult T-Cell Leukemia/Lymphoma (ATL) Cells and Search for ATL-Initiating Cell Markers.（ポスター）	Ishigaki T, Kobayashi S, Ohno N, Nakano N, Utsunomiya A, Yamazaki S, Watanabe N, Uchimaru K, Tojo A, Nakauchi H.	The 56th ASH Annual Meeting and Exposition.	2014年12月6日~9日	国外
Clinical features of adult T-cell leukemia/lymphoma (ATL) in Okinawa Prefecture（口演）	Nishi Y, Fukushima T, Nomura S, Tomoyose T, Nakachi S, Morichika K, Tedokon I, Tamaki K, Shimabukuro N, Taira N, Miyagi T, Karimata K, Yohama M, Yamanoha A, Tamaki K, Hayashi M, Arakaki H, Uchihara J, Ooshiro K, Asakura Y, Tanaka Y, Masuzaki H	第76回日本血液学会学術総会	2014年10月31日～11月2日	国内

２．学会誌・雑誌等における論文掲載

掲載した論文（発表題目）	発表者氏名	発表した場所（学会誌・雑誌等名）	発表した時期	国内・外の別
CADM1 expression and stepwise downregulation of CD7 are closely associated with clonal expansion of HTLV-I-infected cells in adult T-cell leukemia/lymphoma.	Kobayashi S, Nakano K, Watanabe E, Ishigaki T, Ohno N, Yuji K, Oyaizu N, Asanuma S, Yamagishi M, Yamochi T, Watanabe N, Tojo A, Watanabe T, Uchimaru K.	Clin Cancer Res	2014.Jun	国外
Human T-cell lymphotropic virus type I-associatedadult T-cell leukemia-lymphoma.	Tsukasaki K, Tobinai K.	Clin Cancer Res	2014.Oct	国外
Molecular Characterization of Chronic-type Adult T-cell Leukemia/Lymphoma.	Yoshida N, Karube K, Utsunomiya A, Tsukasaki K, Imaizumi Y, Taira N, Uike N, Umino A, Arita K, Suguro M, Tsuzuki S, Kinoshita T, Ohshima K, Seto M.	Cancer Res	2014.Oct	国外

Japan Clinical Oncology Group prognostic index and characterization of long-term survivors of aggressive adult T-cell leukemia-lymphoma (JCOG0902A).	Fukushima T, Nomura S, Shimoyama M, Shibata T, Imaizumi Y, Moriuchi Y, Tomoyose T, Uozumi K, Kobayashi Y, Fukushima N, Utsunomiya A, Tara M, Nosaka K, Hidaka M, Uike N, Yoshida S, Tamura K, Ishitsuka K, Kurosawa M, Nakata M, Fukuda H, Hotta T, Tobinai K, Tsukasaki K.	Clin Cancer Res	2014.Sep	国外

Published OnlineFirst April 11, 2014; DOI: 10.1158/1078-0432.CCR-13-3169

Human Cancer Biology

Clinical Cancer Research

CADM1 Expression and Stepwise Downregulation of CD7 Are Closely Associated with Clonal Expansion of HTLV-I–Infected Cells in Adult T-cell Leukemia/Lymphoma

Seiichiro Kobayashi[1], Kazumi Nakano[5], Eri Watanabe[2], Tomohiro Ishigaki[2], Nobuhiro Ohno[3], Koichiro Yuji[3], Naoki Oyaizu[4], Satomi Asanuma[5], Makoto Yamagishi[5], Tadanori Yamochi[5], Nobukazu Watanabe[2], Arinobu Tojo[1,3], Toshiki Watanabe[5], and Kaoru Uchimaru[3]

Abstract

Purpose: Cell adhesion molecule 1 (CADM1), initially identified as a tumor suppressor gene, has recently been reported to be ectopically expressed in primary adult T-cell leukemia–lymphoma (ATL) cells. We incorporated CADM1 into flow-cytometric analysis to reveal oncogenic mechanisms in human T-cell lymphotrophic virus type I (HTLV-I) infection by purifying cells from the intermediate stages of ATL development.

Experimental Design: We isolated CADM1- and CD7-expressing peripheral blood mononuclear cells of asymptomatic carriers and ATLs using multicolor flow cytometry. Fluorescence-activated cell sorted (FACS) subpopulations were subjected to clonal expansion and gene expression analysis.

Results: HTLV-I–infected cells were efficiently enriched in CADM1^{+} subpopulations (D, CADM1^{pos} CD7^{dim} and N, CADM1^{pos}CD7^{neg}). Clonally expanding cells were detected exclusively in these subpopulations in asymptomatic carriers with high proviral load, suggesting that the appearance of D and N could be a surrogate marker of progression from asymptomatic carrier to early ATL. Further disease progression was accompanied by an increase in N with a reciprocal decrease in D, indicating clonal evolution from D to N. The gene expression profiles of D and N in asymptomatic carriers showed similarities to those of indolent ATLs, suggesting that these subpopulations represent premalignant cells. This is further supported by the molecular hallmarks of ATL, that is, drastic downregulation of miR-31 and upregulation of abnormal *Helios* transcripts.

Conclusion: The CADM1 versus CD7 plot accurately reflects disease progression in HTLV-I infection, and CADM1^{+} cells with downregulated CD7 in asymptomatic carriers have common properties with those in indolent ATLs. *Clin Cancer Res; 20(11); 2851–61. ©2014 AACR.*

Introduction

Human T-cell lymphotrophic virus type I (HTLV-I) is a human retrovirus that causes HTLV-I–associated diseases, such as adult T-cell leukemia–lymphoma (ATL), HTLV-I–associated myelopathy/tropical spastic paraparesis, and HTLV-I uveitis (1–3). In Japan, the estimated lifetime risk of developing ATL in HTLV-I carriers is 6% to 7% for males and 2% to 3% for females (4–6). It takes several decades for HTLV-I–infected cells to reach the final stage of multistep oncogenesis, which is clinically recognized as aggressive ATL (acute-type and lymphoma-type; ref. 7). Molecular interaction of viral genes [e.g., Tax and the HTLV-I basic leucine zipper (HBZ) gene] with the cellular machinery causes various genetic and epigenetic alterations (7–11). However, difficulties in purifying HTLV-I–infected cells *in vivo* seem to have hindered understanding of the genetic events that are directly involved in the multistep oncogenesis of ATL.

Upregulation or aberrant expression of cell surface markers, such as CCR4 and CD25, is useful for diagnosis of ATL and has been utilized for molecular-targeted therapy (12, 13). However, the expression levels of these markers vary among patients, which often make it difficult to identify ATL cells specifically based on the immunophenotype. Previously, we focused on downregulated markers in acute-type ATL cells, such as CD3 and CD7, and successfully purified ATL cells using the CD3 versus CD7 plot of CD4^{+} cells (14). Analysis of other clinical subtypes

Authors' affiliations: [1]Division of Molecular Therapy; [2]Laboratory of Diagnostic Medicine, Division of Stem Cell Therapy; [3]Department of Hematology/Oncology, Research Hospital; [4]Clinical Laboratory, Research Hospital, Institute of Medical Science; and [5]Graduate School of Frontier Sciences, The University of Tokyo, Tokyo, Japan

Note: Supplementary data for this article are available at Clinical Cancer Research Online (http://clincancerres.aacrjournals.org/).

Corresponding Author: Kaoru Uchimaru, Institute of Medical Science, The University of Tokyo, 4-6-1 Shirokanedai, Minato-ku, Tokyo 108-8639, Japan. Phone: 81-3-5449-5542; Fax: 81-3-5449-5429; E-mail: uchimaru@ims.u-tokyo.ac.jp

doi: 10.1158/1078-0432.CCR-13-3169

Published OnlineFirst April 11, 2014; DOI: 10.1158/1078-0432.CCR-13-3169

Translational Relevance

In this study, we showed that the cell adhesion molecule 1 (CAMD1) versus CD7 plot reflects the progression of disease in patients infected with human T-cell lymphotrophic virus type I (HTLV-I), in that the proportion of CADM1^{+} subpopulations (D, CADM1^{pos} CD7^{dim} and N, CADM1^{pos}CD7^{neg}) increased with the progression from HTLV-I asymptomatic carrier (AC) to indolent adult T-cell leukemia–lymphoma (ATL) to aggressive ATL. We confirmed the purity of the clonal HTLV-I–infected cells in these subpopulations of various clinical subtypes, including asymptomatic carriers. The results from the flow-cytometric analysis will help physicians assess disease status. The analysis is also practical in screening for putative high-risk HTLV-I asymptomatic carriers, which show nearly identical flow-cytometric and gene expression profiles with those of smoldering-type ATL patients. Furthermore, cell sorting by flow cytometry enables purification of clonally expanding cells in various stages of oncogenesis in the course of progression to aggressive ATL. Detailed molecular analysis of these cells will provide valuable information about the molecular events involved in multistep oncogenesis of ATL.

(indolent ATLs and HTLV-I asymptomatic carriers; AC) revealed that HTLV-I–infected and clonally expanded cells were purified similarly and that the subpopulations with downregulated CD7 grew concomitantly with the progression of HTLV-I infection (15). Although this type of flow-cytometric analysis was shown to be a useful tool, a substantial subpopulation of T cells shows downregulated expression of CD7 under physiologic (16, 17) and certain pathologic conditions, including autoimmune disorders, viral infection, and hematopoietic stem cell transplantation (18–23).

Recently, Sasaki and colleagues reported ectopic overexpression of the cell adhesion molecule 1/tumor suppressor in lung cancer 1 (CADM1/TSLC1) gene in primary acute-type ATL cells based on expression profile analysis (24, 25). CADM1 (/TSLC1) is a cell-adhesion molecule that was originally identified as a tumor suppressor in lung cancers (25, 26). In addition, numbers of CD4^{+} CADM1^{+} cells have been found to be significantly correlated with the proviral load (PVL) in both ATLs and HTLV-I asymptomatic carriers (25, 27). Thus, CADM1 is a good candidate marker of HTLV-I–infected cells. In the present study, we incorporated CADM1 into our flow-cytometric analysis. In the CADM1 versus CD7 plot of CD4^{+} cells, HTLV-I–infected and clonally expanded cells were efficiently enriched in the CADM1^{+} subpopulations regardless of disease status. In these cells, stepwise CD7 downregulation (from dimly positive to negative) occurred with disease progression. The proportion of the three subpopulations observed in this plot [P, CADM1$^{negative(neg)}$CD7$^{positive(pos)}$; D, CADM1^{pos}CD7^{dim}; and N, CADM1^{pos} CD7^{neg}] accurately reflected the disease status in HTLV-I infection. The analysis of comprehensive gene expression in each subpopulation revealed that the expression profile of CADM1^{+} subpopulations in indolent ATLs showed similarities with that in asymptomatic carriers with high PVL; yet, it was distinct from that in aggressive ATLs. These D and N subpopulations were indicative of HTLV-I–infected cells in the intermediate stage of ATL development.

Materials and Methods

Cell lines and patient samples

TL-Om1, an HTLV-I–infected cell line (28), was provided by Dr. Sugamura (Tohoku University, Sendai, Japan). The MT-2 cell line was a gift from Dr. Miyoshi (Kochi University, Kochi, Japan) and ST-1 was from Dr. Nagai (Nagasaki University, Nagasaki, Japan). Peripheral blood samples were collected from in-patients and out-patients at our hospital, as described in our previous reports (14, 15). As shown in Supplementary Table S1, 26 cases were analyzed (10 cases of asymptomatic carrier; 5 cases of smoldering-type; 6 cases of chronic-type; and 5 cases of acute-type). All patients with ATL were categorized into clinical subtypes according to Shimoyama's criteria (12, 29). Patients with various complications, such as autoimmune disorders and systemic infections, were excluded. Lymphoma-type patients were also excluded because ATL cells are not considered to exist in the peripheral blood of this clinical subtype. Samples collected from six healthy volunteers (mean age 48.8 years; range 34–66 years) were used as normal controls. The present study was approved by the Institutional Review Board of our institute (the University of Tokyo, Tokyo, Japan). Written informed consent was obtained from all patients and healthy volunteers.

Flow cytometry and cell sorting

Peripheral blood mononuclear cells (PBMC) were isolated from whole blood by density gradient centrifugation, as described previously (14). An unlabeled CADM1 antibody (clone 3E1) and an isotype control chicken immunoglobulin Y (IgY) antibody were purchased from MBL. These were biotinylated (primary amine biotinylation) using biotin N-hydroxysuccinimide ester (Sigma-Aldrich). Pacific Orange-conjugated anti-CD14 antibody was purchased from Caltag-Invitrogen. All other antibodies were obtained from BioLegend. Cells were stained using a combination of biotin-CADM1, allophycocyanin (APC)-CD7, APC-Cy7-CD3, Pacific Blue-CD4, and Pacific Orange-CD14. After washing, phycoerythrin-conjugated streptavidin was applied. Propidium iodide (Sigma-Aldrich) was added to the samples to stain dead cells immediately before flow cytometry. A FACSAria instrument (BD Immunocytometry Systems) was used for all multicolor flow cytometry and fluorescence-activated cell sorting (FACS). Data were analyzed using FlowJo software (TreeStar). The gating

Published OnlineFirst April 11, 2014; DOI: 10.1158/1078-0432.CCR-13-3169

procedure for a representative case is shown in Supplementary Fig. S1.

Quantification of HTLV-I proviral load by real-time quantitative PCR

PVL in FACS-sorted PBMCs was quantified by real-time quantitative PCR (TaqMan method) using the ABI Prism 7000 sequence detection system (Applied Biosystems), as described previously (14, 30).

Evaluation of HTLV-I *HBZ* gene amplification by semiquantitative PCR

HTLV-I *HBZ* gene amplification was performed as described previously (25). Briefly, the 25-μL PCR mixture consisted of 20 pmol of each primer, 2.0 μL of mixed deoxynucleotide triphosphates (2.5 mmol/L each), 2.5 μL of 10× PCR buffer, 1.5 μL of $MgCl_2$ (25 mmol/L), 0.1 μL of AmpliTaq Gold DNA Polymerase (Applied Biosystems), and 20 ng of DNA extracted from cell lines and clinical samples. The PCR consisted of initial denaturation at 94°C for 9 minutes, 30 cycles of 94°C for 30 seconds, 57°C for 30 seconds, and 72°C for 45 seconds, followed by 72°C for 5 minutes. The β-actin gene (*ACTB*) was used as an internal reference control. The primer sequences used were as follows: HBZ forward, 5′-CGCTGCCGATCACGATG-3′; HBZ reverse, 5′-GGAGGAATTGGTGGACG-3′; ACTB forward, 5′-CGTGCTCAGGGCTTCTT-3′; and ACTB reverse, 5′-TGAAGGTCTCAAACATGATCTG-3′. Amplification with these pairs of oligonucleotides yielded 177-bp HBZ and 731-bp β-actin fragments.

FISH for quantification of HTLV-I–infected cells

FISH analysis was performed to detect HTLV-I proviral DNA in mononuclear cells that had been FACS-sorted on the basis of the CADM1 versus CD7 plot. These samples were sent to a commercial laboratory (Chromosome Science Labo Inc.), where FISH analysis was performed. Briefly, pUC/HTLV-I plasmid containing the whole-HTLV-I genome was labeled with digoxigenin by the nick translation method, and was then used as a FISH probe. Pretreatment, hybridization, and washing were performed according to standard laboratory protocols. To remove fluorochrome-labeled antibodies attached to the cell surface, pretreatment consisted of treatment with 0.005% pepsin and 0.1 N HCl. The FISH probe was detected with Cy3-labeled anti-digoxigenin antibody. Cells were counterstained with 4′, 6 diamidino-2-phenylindole. The results were visualized using a DMRA2 conventional fluorescence microscope (Leica) and photographed using a Leica CW4000 cytogenetics workstation. Hybridization signals were evaluated in approximately 100 nuclei.

Inverse long PCR to assess the clonality of HTLV-I–infected cells

For clonality analysis, inverse long PCR was performed as described previously (14). First, 1 μg genomic DNA extracted from the FACS-sorted cells was digested with *Pst*I or *Eco*RI at 37°C overnight. RNase A (Qiagen) was added to remove residual RNA completely. DNA fragments were purified using a QIAEX2 Gel Extraction Kit (Qiagen). The purified DNA was self-ligated with T4 DNA ligase (Takara Bio) at 16°C overnight. After ligation of the *Eco*RI-digested samples, the ligated DNA was further digested with *Mlu*I, which cuts the pX region of the HTLV-I genome and prevents amplification of the viral genome. Inverse long PCR was performed using Tks Gflex DNA Polymerase (Takara Bio). For the *Pst*I-treated group, the forward primer was 5′-CAGCCCATTCTATAGCACTCTCCAGGAGAG-3′ and the reverse primer was 5′-CAGTCTCCAAACACGTAGACTGGGTATCCG-3′. For the *Eco*RI-treated template, the forward primer was 5′-TGCCTGACCCTGCTTGCTCAACTCTACGTCTTTG-3′ and the reverse primer was 5′-AGTCTGGGCCCTGACCTTTTCAGACTTCTGTTTC-3′. Processed genomic DNA (50 ng) was used as a template. The reaction mixture was subjected to 35 cycles of denaturation (94°C, 30 seconds) and annealing plus extension (68°C, 8 minutes). Following PCR, the products were subjected to electrophoresis on 0.8% agarose gels. Fourteen patient samples were analyzed. For samples from which a sufficient amount of DNA was extracted, PCR was generally performed in duplicate.

Gene expression microarray analysis of each subpopulation in the CADM1 versus CD7 plot

Total RNA was extracted from each subpopulation in the CADM1 versus CD7 plot using TRIzol (Invitrogen) according to the manufacturer's protocol. Details of the clinical samples used for microarray analyses are shown in Supplementary Table S1. Treatment with DNase I (Takara Bio) was conducted to eliminate genomic DNA contamination. The quality of the extracted RNA was assessed using a BioAnalyzer 2000 system (Agilent Technologies). The RNA was then Cy3-labeled using a Low Input Quick Amp Labeling Kit (Agilent Technologies). Labeled cRNA samples were hybridized to 44K Whole Human Genome Oligonucleotide Microarrays (Agilent Technologies) at 65°C for 17 hours. After hybridization, the microarrays were washed and scanned with a Scanner C (Agilent Technologies). Signal intensities were evaluated by Feature Extraction 10.7 software and then analyzed using Gene Spring 12.0 software (Agilent Technologies). Unsupervised two-dimensional hierarchical clustering analysis (Pearson correlation) was performed on 10,278 genes selected by one-way ANOVA ($P < 0.05$). The dataset for these DNA microarrays has been deposited in Gene Expression Omnibus (accession number GSE55851).

Expression analysis of miR-31 and *Helios* transcript variants of each subpopulation in the CADM1 versus CD7 plot

The expression levels of the microRNA miR-31 were quantified using a TaqMan-based MicroRNA Assay (Applied Biosystems), as described previously (31), and normalized to RNU48 expression level. Helios mRNA transcript variants were examined using reverse transcription

Published OnlineFirst April 11, 2014; DOI: 10.1158/1078-0432.CCR-13-3169

PCR (RT-PCR) with Platinum Taq DNA Polymerase High Fidelity (Invitrogen), as described previously (32). To detect and distinguish alternative splicing variants, PCR analyses were performed with sense and antisense primer sets specific for the first and final exons of the Helios gene. The PCR products were then sequenced to determine the exact type of transcript variant. A mixture of Hel-1, Hel-2, Hel-5, and Hel-6 cDNA fragments was used as a "Helios standard" in the electrophoresis of RT-PCR samples.

Results

CADM1 expression based on the CD3 versus CD7 plot in CD4$^+$ cells in primary HTLV-I–infected blood samples

The clinical profiles of the 32 cases analyzed are shown in Supplementary Table S1. We first examined CADM1 expression in each subpopulation (H, I, and L) of the CD3 versus CD7 plot. Representative data (for a case of smoldering ATL) are shown in Fig. 1A. The results demonstrate that

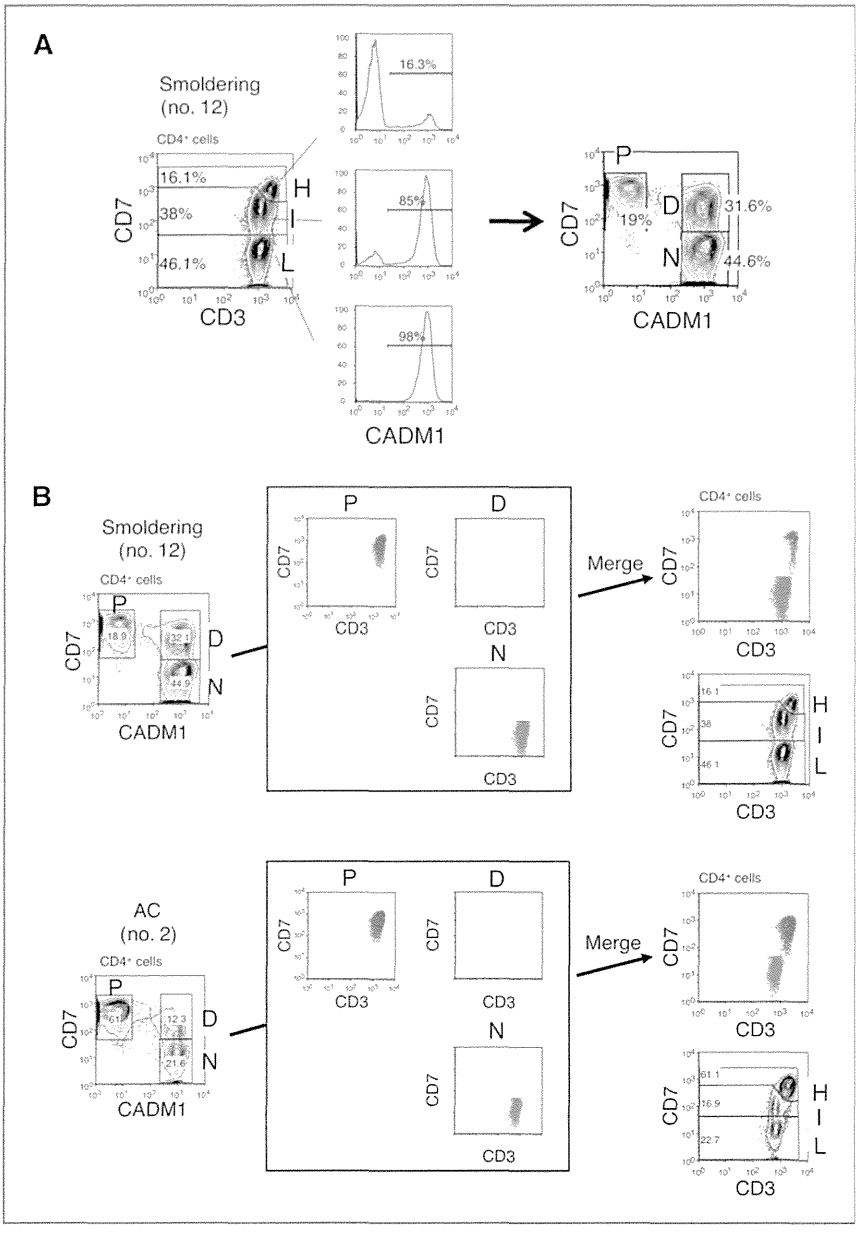

Figure 1. CADM1 versus CD7 plot for CD4$^+$ cells from HTLV-I–infected blood samples analyzed by flow cytometry. A, representative flow-cytometric analysis of a patient with smoldering-type ATL. Three subpopulations (H, I, and L) were observed in the CD3 versus CD7 plot for CD4$^+$ cells (left). Expression of CADM1 in each subpopulation is shown (middle). The right-hand panel shows how the CADM1 versus CD7 plot for CD4$^+$ cells was constructed. B, the P, D, and N subpopulations in the CADM1 versus CD7 plot correspond to the H, I, and L subpopulations in the CD3 versus CD7 plot. Blue, yellow, and red dots, respectively, indicate the P, D, and N subpopulations in the CADM1 versus CD7 plot, and are redrawn in the CD3 versus CD7 plot. Two representative cases are shown. In the upper case, the P and D subpopulations in the CADM1 versus CD7 plot are partly intermingled in the CD3 versus CD7 plot. Unlike the CD3 versus CD7 plot, the CADM1 versus CD7 plot clearly distinguishes three subpopulations.

Published OnlineFirst April 11, 2014; DOI: 10.1158/1078-0432.CCR-13-3169

CADM1 was expressed almost exclusively in the I and L subpopulations. Drawing a CADM1 versus CD7 plot for $CD4^+$ cells revealed three distinct subpopulations (P, $CADM1^{neg}CD7^{pos}$; D, $CADM1^{pos}CD7^{dim}$; and N, $CADM1^{pos}$ $CD7^{neg}$). As shown in Fig. 1B, the P, D, and N subpopulations corresponded to the H, I, and L subpopulations in the CD3 versus CD7 plot. In the previous CD3 versus CD7 plot, the lower case (AC no. 2) showed three distinct subpopulations. However, in the upper case (smoldering no. 12), the H and I subpopulations substantially intermingled with each other and were not clearly separated. In contrast, the CADM1 versus CD7 plot clearly revealed three distinct subpopulations in both cases.

HTLV-I–infected cells are highly enriched in $CADM1^+$ subpopulations

On the basis of previous reports (25, 27), we expected HTLV-I–infected cells to be enriched in the $CADM1^+$ subpopulations in our analysis. Figure 2A shows the PVL measurements of the three subpopulations in the CADM1 versus CD7 plot for three representative cases. HTLV-I–infected cells were highly enriched in the $CADM1^+$ subpopulations (D and N). The PVL data indicate that most of the cells in the D and N subpopulations were HTLV-I infected. Figure 2B shows the results of semiquantitative PCR of the *HBZ* gene in representative cases. In the D and N subpopulations, the *HBZ* gene was amplified to the same degree as in the HTLV-I–positive cell line. To confirm these results, FISH was performed in one asymptomatic carrier. As shown in Supplementary Fig. S2, HTLV-I–infected cells were highly enriched in the D and N subpopulations, which supports the results of the PVL analysis and semiquantitative PCR of the *HBZ* gene. In the FISH analysis, percentages of HTLV-I–infected cells in D and N did not reach 100%. This may have been due to a technical issue. Because the cells subjected to FISH analysis were sorted by FACS, several fluorochrome-conjugated antibodies may have remained on their surfaces, even after treatment with protease.

The CADM1 versus CD7 plot accurately reflects disease progression in HTLV-I infection

Compared with the CD3 versus CD7 plot, the CADM1 versus CD7 plot was revealed to be clear in its distinction of the three subpopulations and efficient in enrichment of HTLV-I–infected cells. On the basis of these findings, we analyzed clinical samples of asymptomatic carriers and three clinical subtypes of ATL: the smoldering, chronic, and acute subtypes. Data for representative cases, presented in Fig. 3A, suggest that the continual changes in the proportions of the three subpopulations are associated with disease progression. In the CADM1 versus CD7 plot, normal control samples showed a P-dominant pattern. With progression of the disease from the asymptomatic carrier state with a low PVL to that with a high PVL, and to indolent-type ATL, the D and N subpopulations increased gradually. As the disease further progressed to acute-type ATL, the N subpopulation showed remarkable expansion. Data for all analyzed samples are presented in Fig. 3B. The results suggest that the CADM1 versus CD7 plot of peripheral blood samples represents progression of the disease in HTLV-I carriers. Data for the normal control cases analyzed are shown in Supplementary Fig. S3. In all normal controls, the percentages of the D and N subpopulations were low. Supplementary Fig. S4 shows temporal data for a patient with chronic-type ATL who progressed from stable disease to a relatively progressive state and the concomitant change in the flow cytometry profile.

Clonality analysis of the three subpopulations in the CADM1 versus CD7 plot

To characterize the three subpopulations further, the clonal composition of each subpopulation was analyzed by inverse long PCR, which amplifies part of the provirus

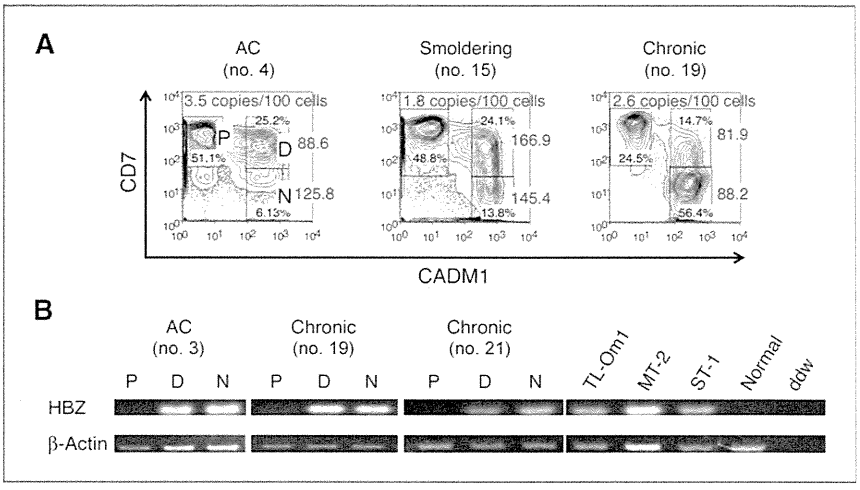

Figure 2. HTLV-I–infected cells are highly enriched in the $CADM1^+$ subpopulations. A, analysis of PVL in the three subpopulations. Three representative cases are shown. PVL data (copies/100 cells) are shown in red. Percentages of each subpopulation are shown in black. B, semiquantitative PCR of the *HBZ* gene in the three subpopulations in three representative cases. Normal, DNA from PBMCs from a normal control; ddw, deionized distilled water.

Published OnlineFirst April 11, 2014; DOI: 10.1158/1078-0432.CCR-13-3169

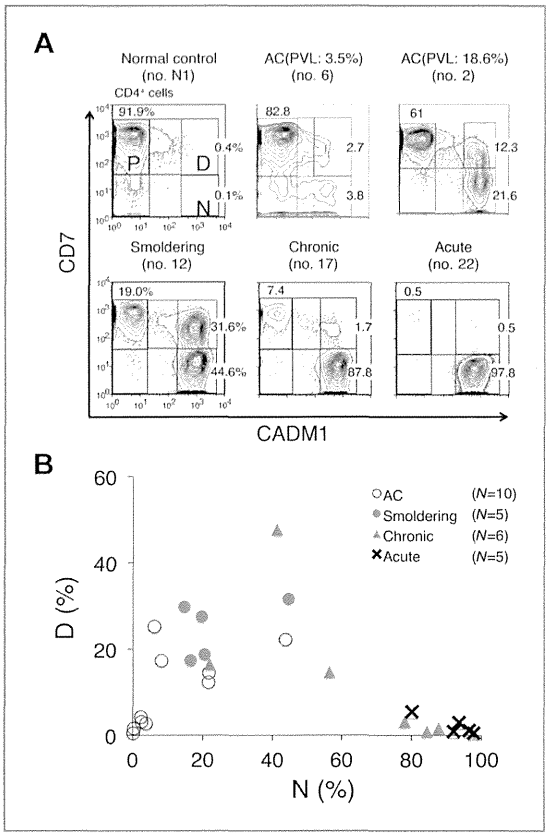

Figure 3. Proportion of each subpopulation in the CADM1 versus CD7 plots for asymptomatic HTLV-I carriers (asymptomatic carriers) and ATLs of various clinical subtypes. A, data of representative cases are shown. B, a two-dimensional plot of all analyzed samples showing the percentages of the D and N subpopulations.

long terminal repeat and the flanking genomic sequence of the integration sites. Cells in each subpopulation were sorted by FACS, and subjected to inverse long PCR analysis. Representative results for smoldering-, chronic-, and acute-type ATL samples are presented in Fig. 4A. Major clones, indicated by intense bands, were detected in the D and N subpopulations. The major clones in the D and N subpopulations in each case were considered to be the same based on the sizes of the amplified bands, suggesting that clonal evolution is accompanied by downregulation of CD7 expression. Fig. 4B shows representative results for three cases of asymptomatic carrier. In all cases, weak bands in the P subpopulation were visible, indicating that this population contains only minor clones. In these asymptomatic carriers, the proportion of abnormal lymphocytes and PVL increases from left to right. The consistent increase in the D and N subpopulations, together with growth of major clones as shown in the inverse PCR analysis, were considered to reflect these clinical data.

Gene expression profiling of the three subpopulations in the CADM1 versus CD7 plot

To determine the molecular basis for the biologic differences among the three subpopulations in the CADM1 versus CD7 plot, we next characterized the gene-expression profiles of the subpopulations of the following clinical subgroups: asymptomatic carriers ($n = 2$), smoldering-type ATLs ($n = 2$), chronic-type ATL ($n = 1$), acute-type ATLs ($n = 3$), and normal controls ($n = 3$). The two asymptomatic carriers (nos. 5 and 9) had high PVLs (11.6 and 26.2%, respectively) and relatively high proportions of D and N subpopulations (Supplementary Table S1). Unsupervised hierarchical clustering analysis of the results revealed three clusters (A, B1, and B2) or two major clusters A and B, where A is composed solely of the samples of the acute-type N subpopulation and B is subdivided into two clusters (B1 and B2; Fig. 5A). The B2 cluster is composed of the P subpopulation of all clinical subtypes and of normal controls, whereas the B1 cluster is composed of the D and N subpopulations of

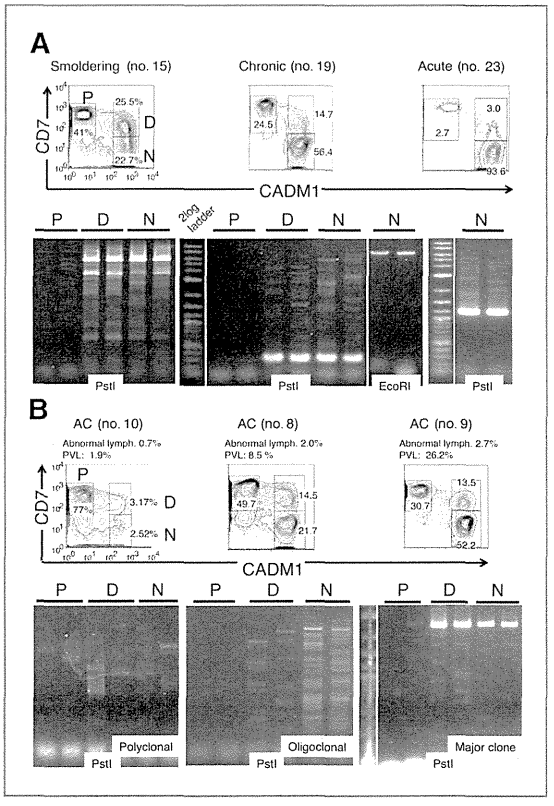

Figure 4. Clonality of subpopulations in the CADM1 versus CD7 plot analyzed by inverse long PCR. FACS-sorted cells (P, D, and N) were subjected to inverse long PCR. The black bar indicates duplicate data. Flow-cytometric profiles and clinical data are also presented. A, representative cases of smoldering-, chronic-, and acute-type ATL are shown. B, representative cases of asymptomatic carriers are shown.

Published OnlineFirst April 11, 2014; DOI: 10.1158/1078-0432.CCR-13-3169

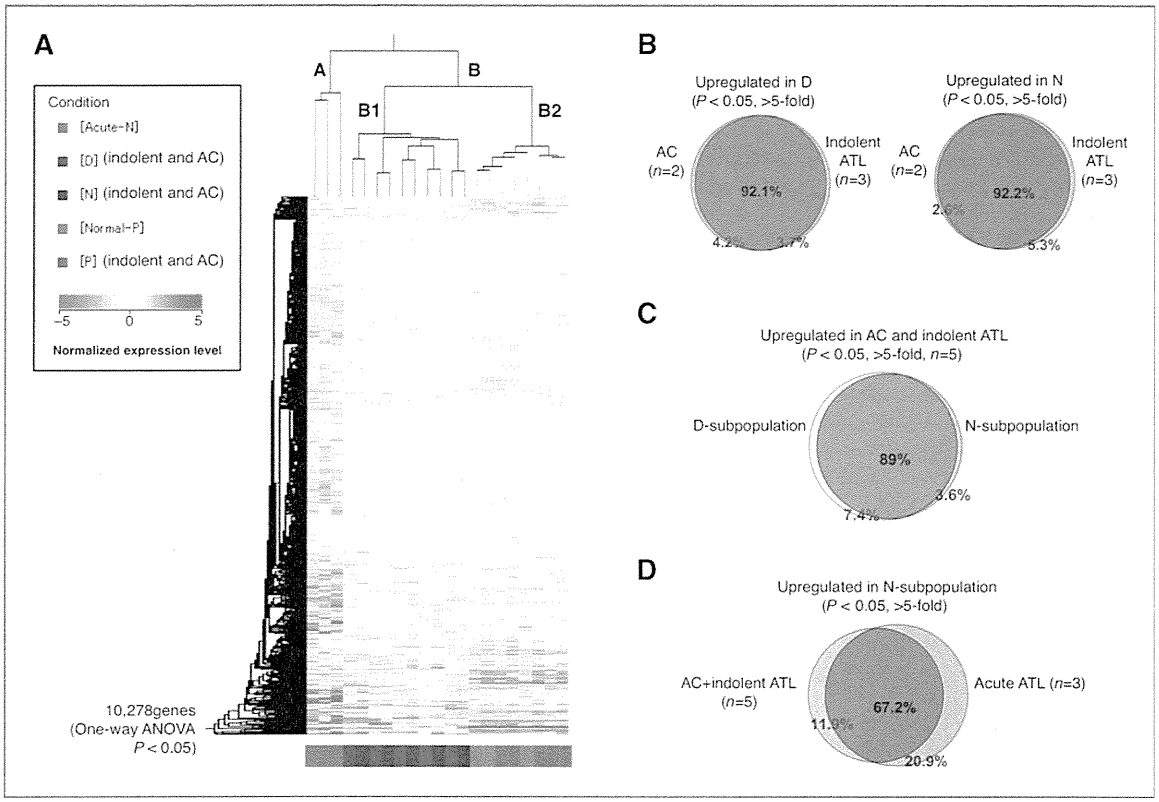

Figure 5. Comprehensive gene expression analysis of the three subpopulations in the CADM1 versus CD7 plot. A, we conducted an unsupervised hierarchical clustering analysis of 10,278 genes whose expression levels were significantly changed in the P subpopulation of normal controls ($n = 3$); P, D, and N subpopulations of asymptomatic carriers and indolent ATLs ($n = 5$); and N subpopulation of acute-ATLs ($n = 3$; one-way ANOVA, $P < 0.05$). The P and D subpopulations of acute ATLs and D and N subpopulations of normal controls could not be analyzed because of insufficient numbers of cells. Clustering resulted in three major clusters: (i) P subpopulations of normal controls (gray) and asymptomatic carriers/indolent ATLs (green); (ii) D and N subpopulations of asymptomatic carriers/indolent ATLs (blue and brown, respectively); and (iii) N subpopulations of acute ATLs (red). These results indicate that the P subpopulations of asymptomatic carriers/indolent ATLs have characteristics similar to those of normal uninfected cells, whereas the D and N subpopulations of asymptomatic carriers/indolent ATLs have genetic lesions in common. The N subpopulations of acute ATLs are grouped in an independent cluster, meaning that these malignant cell populations have a significantly different gene expression profile, even compared with the N subpopulations of indolent ATLs. B, similarity between asymptomatic carriers and indolent ATLs. The Venn diagrams show that 92.1% and 92.2% of genes upregulated in the D and N subpopulations, respectively, compared with "Normal-P" ($P < 0.05$), were common to asymptomatic carriers ($n = 2$) and indolent ATLs ($n = 3$). C, similarity between the D and N subpopulations. The Venn diagram shows that 89% of genes upregulated in the D and N subpopulation, compared with Normal-P ($P < 0.05$), overlapped. D, comparison of the N subgroups between acute-ATLs ($n = 3$) and asymptomatic carriers/indolent ATLs ($n = 5$). As shown in the Venn diagram, 67.2% of genes were upregulated ($P < 0.05$) in the N subpopulations of both acute ATLs and asymptomatic carrier/indolent ATLs. However, a significant number of genes (20.9%) were upregulated only in the N subpopulation of acute ATLs.

asymptomatic carriers and indolent ATLs (smoldering- and chronic-type).

Figure 5B shows a Venn diagram of the upregulated genes in the D subpopulation (left) or the N subpopulation (right) common to asymptomatic carriers ($n = 2$) and indolent ATLs ($n = 3$). These diagrams demonstrate that the changes in the gene expression profiles of the D and N subpopulations of asymptomatic carriers were similar to those of indolent ATLs. Furthermore, the gene expression profiles of the D and N subpopulations of asymptomatic carriers and indolent ATLs were similar (Fig. 5C). In contrast, the upregulated genes showed distinct differences between the N subpopulation of acute-type ATL and that of indolent ATLs and asymptomatic carriers, although approximately 70% were common to both (Fig. 5D).

Expression of a tumor suppressor microRNA and splicing abnormalities of Ikaros family genes in the three subpopulations

To determine whether the novel subpopulations identified had other properties in common with ATL cells, we examined miR-31 levels and *Helios* mRNA patterns in sorted subpopulations (31, 32). Expression of miR-31 decreased drastically in the D subpopulation derived from indolent ATLs and asymptomatic carriers, and was